Spectrum of Passive Scalar at Very High Schmidt Number in Turbulence*)

Toshiyuki GOTOH, Takeshi WATANABE and Hideaki MIURA[1)]

Nagoya Institute of Technology, Gokiso, Showa-ku, Nagoya 466-8555, Japan
[1)]*National Institute for Fusion Science, Toki 509-5292, Japan*

(Received 21 November 2013 / Accepted 3 February 2014)

A hybrid code which uses the spectral method for an incompressible fluid and the combined compact finite difference method for passive scalar is developed and applied to compute the spectrum of the passive scalar variance in turbulence at very high Schmidt numbers up to 1000. The accuracy and efficiency of the hybrid code are found to be very satisfactory when compared to the full spectral computation. The scalar spectrum in the viscous-convective range by direct numerical simulation is found to obey k^{-1} power law and to exponentially decay in the far diffusive range, and compared to Kraichnan's spectrum. It is argued that the exponential decay of the spectrum in the far diffusive range is due to the intermittency effect of the velocity field.

© *2014 The Japan Society of Plasma Science and Nuclear Fusion Research*

Keywords: passive scalar spectrum, universality, turbulence, hybrid method, combined compact finite difference

DOI: 10.1585/pfr.9.3401019

1. Introduction

Turbulence is a ubiquitous phenomenon and found in many places in daily life, engineering flow, in the atmosphere and ocean and in space and fusion plasmas. Turbulence is characterized by its large power of transporting heat, mass and momentum and by their strong fluctuations. Since Kolmogorov's theory many efforts have been made to elucidate and explain statistical laws of strong fluctuations as well as the mean properties such as mean velocity. The latter is strongly affected by the macroscopic conditions and thus not universal. On the other hand, small scale motion in turbulent flow is generated through cascade process during which memories at large scales are lost and a universal equilibrium state is achieved. It is known that when the Reynolds number is very high the 4/5 law for the third order moment of the velocity increment is asymptotically exact and that the Kolmogorov constant in the kinetic energy spectrum and the scaling exponents of the moments of the longitudinal velocity increments are little changed for various types of turbulent flows, which means that those statistical quantities are universal.

Problem of passive scalar (no reaction to the velocity field) convected by turbulence is very fundamental and important to the understanding of turbulent mixing phenomena, anomalous transport in turbulence and MHD turbulence. Since the equation for the passive scalar is linear and local in space, the problem has been thought to be more tractable than the turbulent velocity and has attracted many interests from the beginning. However, the experiments and direct numerical simulations (DNSs) have shown that the statistical laws of the passive scalar is not as definite as in the velocity.

The spectrum of the scalar variance is defined by

$$\left\langle \theta^2 \right\rangle = \int_0^\infty E_\theta(k)\,\mathrm{d}k. \tag{1}$$

When the Reynolds number is very high and the Schmidt number $Sc = \nu/\kappa$ is $O(1)$, where ν and κ are the molecular viscosity and the molecular diffusivity, respectively, Okbukhov [1] and Corrsin [2] have independently found that the inertial-convective range exists and the scalar spectrum obeys

$$E_\theta(k) = C_\mathrm{O}\overline{\chi}\,\overline{\epsilon}^{\,-1/3}k^{-5/3}. \tag{2}$$

When $Sc \gg 1$ (the Reynolds numbers is not necessarily high), Batchelor derived the scalar spectrum

$$E_\theta(k) = C_\mathrm{B}\overline{\chi}(\overline{\epsilon}/\nu)^{-1/2}k^{-1}\exp\left(-C_\mathrm{B}(k\eta_\mathrm{B})^2\right), \tag{3}$$

in the viscous-convective range [3, 4], where $\overline{\epsilon}$ and $\overline{\chi}$ are the mean kinetic energy dissipation rate per unit mass and the mean scalar dissipation rate, respectively and $\eta_\mathrm{B} = (\nu\kappa^2/\overline{\epsilon})^{1/4}$ is the Batchelor length. The Obukhov-Corrsin constant C_O and the Batchelor constant C_B are considered to be universal, but the values scatter considerably when compared to the Kolmogorov constant K in the kinetic energy spectrum $E(k) = K\overline{\epsilon}^{2/3}k^{-5/3}$ in the inertial range [4]. The functional form of $E_\theta(k)$ in the far diffusive range when the viscous-convective range exists is not settled. Batchelor predicted a rapid decay in the Gaussian form as in Eq. (3) [3] , while Kraichnan predicted the exponential decay [5–7].

$$E_\theta(k) = C_\mathrm{B}\overline{\chi}(\overline{\epsilon}/\nu)^{-1/2}k^{-1}\left(1+\sqrt{6C_\mathrm{B}}k\eta_\mathrm{B}\right) \times \exp\left(-\sqrt{6C_\mathrm{B}}k\eta_\mathrm{B}\right), \tag{4}$$

author's e-mail: gotoh.toshiyuki@nitech.ac.jp

*) This article is based on the presentation at the 23rd International Toki Conference (ITC23).

© 2014 The Japan Society of Plasma Science and Nuclear Fusion Research

for the velocity field which obeys the multivariate Gaussian statistics and is delta correlated in time [6]. The constant C_B is determined by the Lagrangian spectral theory such as ALHDIA, SBALHDIA, and LRA which do not contain any ad hoc parameters [4, 7], but their predicted values are quite low when compared to the ones obtained by experiments and DNS which scatter considerably too [4]. This shows that even in this simplest problem the scalar spectrum is not well understood. Although the 4/3 law for the third order moment of the squared scalar increment times the velocity increment is asymptotically exact, no exact relation for the statistics consisting of the scalar quantity alone is known. Even the isotropy of the scalar at small scales is questioned, and the scaling exponents of the high order moments of the scalar increments vary from experiments to experiments. These facts raise a question concerning the strength of universality of the passive scalar statistics at small scales. In this context, it is very important and necessary to the understanding of the universality in the scalar turbulence to carefully study the scalar spectrum in an asymptotic state such that a rigorous theory can be established and the numerical computation is as faithful to the assumption used in the theory as possible. In this paper we study the scalar spectrum at very high Schmidt number by using DNS with very high resolution and examine the theoretical prediction.

2. Hybrid Method

Since the universality of the small scale statistics of turbulence and scalar manifests in the asymptotic limit of large Reynolds number or large Schmidt number, the DNS study requires very high resolution in space and time. The high performance computers use a large number of nodes and the conventional spectral method using the Fast Fourier Transform (FFT) has a serious bottleneck in the communication. Therefore more efficient numerical method while keeping the comparable accuracy as the spectral method is highly demanding. For this purpose we have newly developed a hybrid code and applied it to the problem of the passive scalar spectrum in the viscous-convective and far diffusive range at very high Schmidt number.

An idea to develop an efficient code is to anticipate the locality and non-locality of the equations for an incompressible fluid and passive scalar [8]. They are written as

$$\frac{\partial \boldsymbol{u}}{\partial t} + \boldsymbol{u}\cdot\nabla\boldsymbol{u} = -\frac{1}{4\pi}\nabla\int\frac{1}{|\boldsymbol{x}-\boldsymbol{y}|}\nabla\boldsymbol{u}:\nabla\boldsymbol{u}\,\mathrm{d}\boldsymbol{y} + \nu\Delta\boldsymbol{u}, \quad (5)$$

$$\frac{\partial \theta}{\partial t} + \boldsymbol{u}\cdot\nabla\theta = \kappa\Delta\theta, \quad (6)$$

for an infinite domain, where the pressure is eliminated by using the incompressibility condition. Equation (5) is nonlocal in space while the scalar equation (6) is local. The non-local data transfer is unavoidable because of the non-locality of the pressure term whatever the numerical scheme is chosen. Therefore the spectral method is the most accurate method for solving the Poisson equation for the pressure. On the other hand, if we have a suitable differential operator with high accuracy which is effectively comparable to that of the spectral method, it is possible to reduce the amount of data transfer required for the differentiation. For this purpose we have chosen the combined compact finite difference (CCD) method [9–11]. Mixed use of the spectral method for the incompressibility fluid and the CCD method for the passive scalar is called as hybrid method. Highly parallelized code was developed for the three dimensional domain decomposition, and accuracy and performance of the hybrid method were examined in detail in [8].

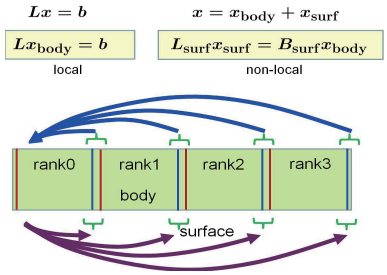

Fig. 1 Schematic picture of solving linear equation for combined compact finite difference method on parallel machine.

Since the computation of the passive scalar problem on the many core machine is communication intensive, it is important to see the cost of the data transfer. Suppose that a cubic domain with size 2π is discretized into N^3 grid points. In the spectral method, the spatial derivative is equivalent to multiplication by $i\boldsymbol{k}$ therefore no data transfer occurs, while it requires $O(N^3)$ data transfer to compute the convective term by using 3DFFT. On the other hand, in the CCD method, to obtain the derivatives means to solve the linear equation $L\boldsymbol{x} = \boldsymbol{b}$. On the parallel computer, we split the solution vector $\boldsymbol{x}$ into two parts as $\boldsymbol{x} = \boldsymbol{x}_{\mathrm{body}} + \boldsymbol{x}_{\mathrm{surf}}$ (see Fig.1) [11]. The vectors $\boldsymbol{x}_{\mathrm{body}}$ and $\boldsymbol{x}_{\mathrm{surf}}$ are the solutions of $L\boldsymbol{x}_{\mathrm{body}} = \boldsymbol{b}$ and $\tilde{L}\boldsymbol{x}_{\mathrm{surf}} = B\boldsymbol{x}_{\mathrm{body}}$, respectively, where the matrices $\tilde{L}$ and B are deduced from L. The first equation is solved within each node so that no data transfer is required, while in the second equation the data $\boldsymbol{x}_{\mathrm{body}}$ at grid points near boundaries of all nodes are gathered on one node, solved and redistributed on each node, thus the nonlocal data transfer of the order of $O(N^2)$ is necessary (Fig. 2). When N is large, the hybrid method for the scalar equation has advantage over the spectral method.

One more thing to be considered is the fact that when the Schmidt number is very high there is the scale separation between the velocity and scalar fields in the viscous-convective range, such that the velocity is so smooth while the scalar field is highly fluctuating. Then it is quite natural to use the coarser mesh for the velocity and the fine mesh for the scalar and the velocity field at the grid points of the scalar is well approximated by the linear or cubic interpolation. The use of dual grid reduces considerably the computational cost.

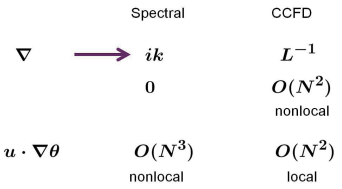

Fig. 2 Estimate of the amount of data transfer in the spectral and CCD methods.

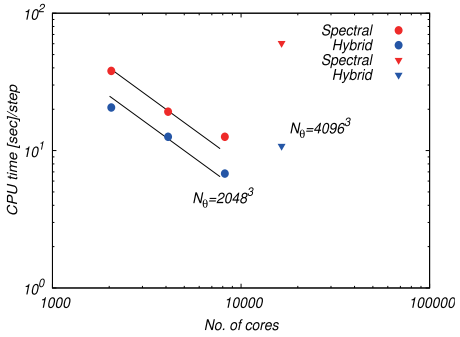

Fig. 3 Comparison of CPU time for spectral and hybrid codes at $Sc = 1000$ measured on Plasma Simulator. In the spectral computation, the numbers of grid points of the velocity and scalar are $N_v = N_\theta = 2048^3$ for red circle and $N_v = N_\theta = 4096^3$ for red triangle. In the hybrid computation, $N_\theta = 2048^3$ for blue circle and $N_\theta = 4096^3$ for blue triangle, and $N_v = 256^3$ for two cases.

A benchmark test of the hybrid method for $Sc = 1000$ is shown in Fig. 3. In the spectral computation, the numbers of grid points of the velocity and scalar are equal and $N_v = N_\theta = 2048^3$ for red circle and $N_v = N_\theta = 4096^3$ for red triangle. In the hybrid computation, $N_\theta = 2048^3$ for blue circle and $N_\theta = 4096^3$ for blue triangle, and $N_v = 256^3$ for two cases. The same width of time increment is used for the velocity and scalar equations. The strong scaling of the code is seen and the acceleration in the computation is enhanced when the number of grid points for the scalar is increased from $N_\theta = 2048^3$ to $N_\theta = 4096^3$. Due to the difference in the scaling of the amount of data transfer, $O(N^3)$ for the spectral method and $O(N^2)$ for the hybrid method, and due to the use of dual grid when the Schmidt number is very high, the advantage of the hybrid method over the spectral method increases with increase of N_θ for a given $N_v (< N_\theta)$. However, it should be noted that this advantage of the hybrid method depends on the performance of the communication of the high performance computer. The above points of the hybrid method applies to the equation which is local in space such as the induction equation for the magnetic field in MHD.

3. Spectrum of Passive Scalar Variance

We have integrated by using the hybrid code a set of equations (5) and (6) to which the Gaussian random force $\boldsymbol{f}$ and scalar injection f_θ are added

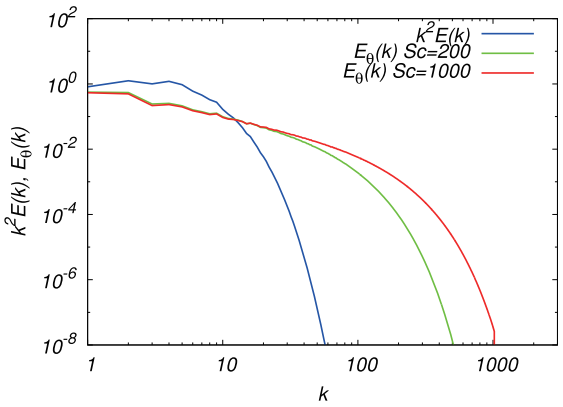

Fig. 4 Averaged enstrophy (blue) and scalar variance spectra in three dimensions for $Sc = 200$ (green) and $Sc = 1000$ (red).

$$\langle \boldsymbol{f}(\boldsymbol{x}, t)\rangle = 0, \tag{7}$$

$$\left\langle f_i(\boldsymbol{x}, t) f_j(\boldsymbol{y}, s)\right\rangle = P_{ij}(\nabla) D(|\boldsymbol{x} - \boldsymbol{y}|)\delta(t - s), \tag{8}$$

$$D(k) = D_0 k^{-1} \ \text{ for } k < 2, \quad D(k) = 0 \ \text{ otherwise}, \tag{9}$$

for the Navier-Stokes equation and

$$\langle f_\theta(\boldsymbol{x}, t)\rangle = 0, \tag{10}$$

$$\langle f_\theta(\boldsymbol{x}, t) f_\theta(\boldsymbol{y}, s)\rangle = D_\theta(|\boldsymbol{x} - \boldsymbol{y}|)\delta(t - s), \tag{11}$$

$$D_\theta(k) = D_0 k^{-1} \ \text{ for } k < 2, \quad D_\theta(k) = 0 \ \text{ otherwise}, \tag{12}$$

for the scalar equation, respectively, where $\langle\ \rangle$ denotes the ensemble average. The Schmidt numbers are 200 and 1000 and the number of grid points are 256^3 for the velocity and 1024^3 at $Sc = 200$ and 2048^3 at $Sc = 1000$ for the passive scalar. The Taylor microscale Reynolds number is kept constant as $R_\lambda = 42$ on average for all the runs. The scalar statistics are gathered and averaged over considerably long time duration. Figure 4 shows the three dimensional spectra of the enstrophy $k^2E(k)$ (blue) and the scalar $E_\theta(k)$ at $Sc = 200$ (green) and 1000 (red). The typical parameters in these computations are $\overline{\epsilon} = 0.250$, $\overline{\chi} = 0.655$, $\eta = 7.52 \times 10^{-2}$, $\eta_B = 5.32 \times 10^{-3}$ for $Sc = 200$ and $\overline{\epsilon} = 0.274$, $\overline{\chi} = 0.628$, $\eta = 7.35 \times 10^{-2}$, $\eta_B = 2.32 \times 10^{-3}$ for $Sc = 1000$, where η and η_B are the Kolmogorov and Batchelor lengths, respectively. It is clearly seen that there is a scale separation between the velocity and scalar and the scalar spectrum has an asymptotic power law range. Figure 5 presents the normalized compensated scalar spectrum $\overline{\chi}^{-1}(\overline{\epsilon}/\nu)^{-1/2} k E_\theta(k)$. The curve at low wavenumber range is horizontal at $C_B = 5.7$ which gives the Batchelor constant. This value is larger than the previously obtained value 4.9 for which the uniform scalar gradient is applied to maintain the scalar field in a statistically steady state [12].

There have been arguments about the spectrum in the far diffusive range when the k^{-1} range exists. As seen in Eqs. (3) and (4), the two theories predict the different behavior of the spectrum in the far diffusive range. In order to examine the spectrum in the far diffusive range, we plotted the one dimensional scalar spectrum

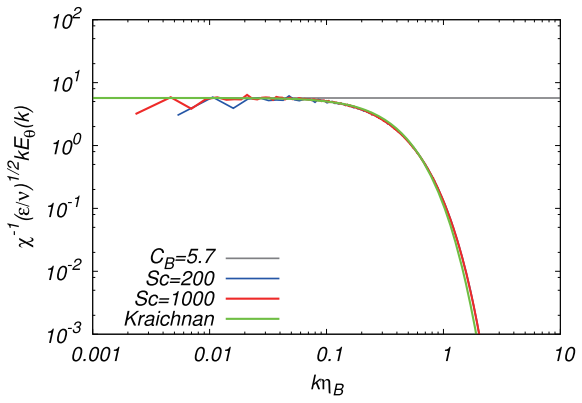

Fig. 5 Comparison of compensated three dimensional scalar variance spectrum at $Sc = 1000$. The Kraichnan spectrum is computed with $C_B = 5.7$.

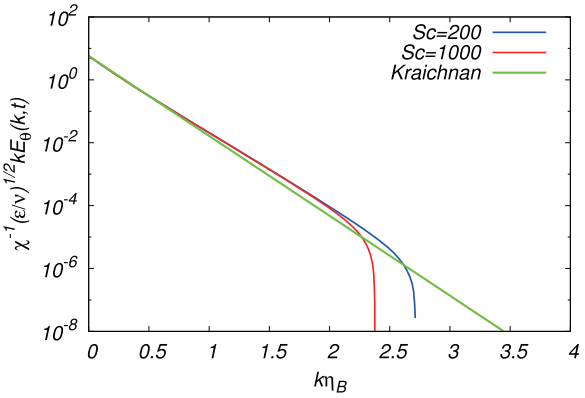

Fig. 6 Comparison of the one dimensional scalar variance spectrum in the far diffusive range at $Sc = 1000$. The Kraichnan spectrum is computed with $C_B = 5.7$.

$$E_{1\theta}(k) = \int_k^\infty \frac{E_\theta(p)}{p}\mathrm{d}p, \tag{13}$$

in Fig. 6. As clearly seen, the curves by DNS and Kraichnan are straight line over the range $0.1 < k\eta_B < 2$, meaning the exponential decay of $E_\theta(k)$ and the slope of the Kraichnan spectrum is slightly steeper than that of DNS. It should be stressed that although both curves are close to each other, the underlining assumption for the velocity, multivariate Gaussian and delta correlated in time, in Kraichnan's theory is totally different from the actual velocity field in DNS for which the velocity is highly non-Gaussian and finitely correlated in time. Therefore physical reason for the exponential decay of $E_\theta(k)$ must be explored.

Batchelor's spectrum Eq. (3) was obtained by considering the balance between the local squeezing motion due to the straining and the molecular diffusive action, $\partial\left[|\gamma|kE_\theta(k)\right]/\partial k = -\kappa k^2 E_\theta(k)$, where $\gamma < 0$ is the smallest eigenvalue of the rate of strain tensor. The solution of this equation is easily obtained as

$$E_\theta(k,\gamma) \propto \frac{1}{|\gamma|k}\exp\left(-\kappa k^2 / |\gamma|\right). \tag{14}$$

He replaced $|\gamma|$ by a representative value as $|\gamma|_{\mathrm{eff}} = C_B(\epsilon/\nu)^{-1/2}$ and obtained Eq. (3). However, the strain fluctuates in space and time and so does for $\gamma(\boldsymbol{x}, t)$. Then it is quite reasonable to take the average over the distribution of γ as $E(k) = \int_{-\infty}^{0} E_\theta(k,\gamma)P(\gamma)\mathrm{d}\gamma$. We have computed the probability density function $P(\gamma)$ by DNS which differs definitely from the one obtained from the Gaussian velocity field, and substituted into the above equation. The obtained results for $E_\theta(k)$ is found to be very close to the spectrum obtained by DNS (figure not shown), which means that the exponential decay of the spectrum is due to the intermittency effects of the velocity strain field.

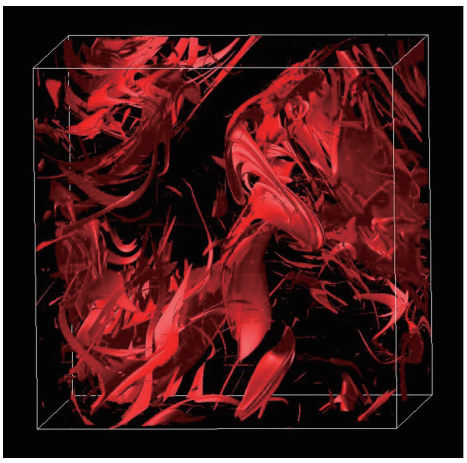

Fig. 7 Visualized scalar field at $Sc = 1000$.

It is interesting to see how the scalar field looks like. Figure 7 shows the scalar field visualized at $Sc = 1000$ computed on $N = 2048^3$ grid points at $R_\lambda = 42$. The scalar field is confined in thin layer and wounded around some axis. The relation to the straining field is the future work.

The authors thank NIFS, HPCI and JHPCN for providing computational resources. Work of T. G and T. W. are supported by Grant-in-Aid for Scientific Research Nos. 24360068 and 23760156, respectively, from the Ministry of Education, Culture, Sports, Science, and Technology of Japan.

[1] A.M. Obukhov, Izv. Akad. Nauk SSSR. Ser. Geogr. Geofiz. **13**, 58 (1949).
[2] S. Corrsin, J. Appl. Phys. **22**, 469 (1951).
[3] G.K. Batchelor, J. Fluid Mech. **5**, 113 (1959).
[4] T. Gotoh and P.K. Yeung, "Passive scalar transport in turbulence" in *Ten Chapters in Turbulence*, P. Davidson, Y. Kaneda and K.R. Sreenivasan Eds., (Cambridge Univ. Press, UK., 2013).
[5] R.H. Kraichnan, Phys. Fluids **11**, 945 (1968).
[6] R.H. Kraichnan, J. Fluid Mech. **64**, 737 (1974).
[7] T. Gotoh, J. Nagaki and Y. Kaneda, Phys. Fluids **12**, 155 (2000).
[8] T. Gotoh, S. Hatanaka and H. Miura, J. Comp. Phys. **231**, 7398 (2012).
[9] S.K. Lele, J. Comp. Phys. **103**, 16 (1992).
[10] P.C. Chu and C. Fan, J. Comp. Phys. **190**, 370 (1998).
[11] T. Nihei and K. Ishii, Theor. Appl. Mech. **52**, 71 (2003).
[12] D.A. Donzis, K.R. Sreenivasan and P.K. Yeung, Flow, Turb. & Combust. **85**, 549 (2010).